PHYSICAL REVIEW B **70**, 165320 (2004)

Nitrogen bonding structure in ultrathin silicon oxynitride films on Si(100) prepared by plasma nitridation

Yu Kwon Kim, Hyun Seok Lee, and H. W. Yeom*
Center for Atomic Wires and Layers and Institute of Physics and Applied Physics, Yonsei University, Seoul, 120-749, Korea

Doo-Yeol Ryoo, Sang-Bum Huh, and Jeong-Gun Lee
Hynix Semiconductor Inc., Cheongju, 361-725, Korea

(Received 1 May 2004; published 27 October 2004)

High-resolution core-level photoemission using synchrotron radiation is applied to the ultrathin SiON films on Si(100) nitrided by N_2 plasma, which gives a systematic view of the various transient or stable N chemical states. N 1*s* spectra disclose at least two characteristic nitrogen bonding states in addition to the well-established and thermally stable $N{\equiv}Si_3$ species. While the stable $N{\equiv}Si_3$ species are located near the interface, the extra high-binding energy states are distributed mainly in the surface region. Among these high-binding species, assigned reliably to the N—O and $N{=}O_2$ bonding states, only the N—O species is quasi-stable up to 900 °C, surviving the post-annealing treatment. These oxidized N species convert to the stable $N{\equiv}Si_3$ mostly within the SiO_2 film. This result indicates that the N—O and $N{=}O_2$ species formed by energetic plasma process is kinetically trapped within the shallow part of the film. It is inferred that the quasi-stable N—O species would play an important role in characterizing the physical and electrical properties of the plasma oxynitrides.

DOI: 10.1103/PhysRevB.70.165320 PACS number(s): 79.60.−i, 81.65.Lp

I. INTRODUCTION

Silicon oxynitride films (SiO_xN_y) have been under intense investigations as a prompt alternative to silicon oxides since they satisfy the requirement of electrical reliability as gate dielectrics for even smaller memory or logic devices within the conventional device-process scheme. By incorporating a small amount of nitrogen into SiO_2, the resulting oxynitride layers are reported to exhibit improved electrical properties and superior interface characteristics such as the suppressed dopant diffusion and the reduced defect generation.[1–3]

So far, various techniques have been developed for nitrogen incorporation including the thermal annealing in NO, N_2O, or N_2 atmosphere[4,5] or the plasma process using similar molecules.[6] The previous investigations showed that the chemical and depth structures of N atoms incorporated in SiO_2 films depend strongly on the nitridation processes. That is, the early studies generally suggested that plasma oxynitrides have a broader N distribution within the oxide[7–9] while thermal oxynitrides have significant nitrogen accumulation in the SiO_2/Si interface.[10,11] In technological aspects, this requires the development and refinement of a proper nitridation process to yield a certain N profile, which is suitable for the functional needs of a specific device structure or performance. At the same time, the fundamental and microscopic understanding of the nitrogen incorporation process itself is very much demanding.

One fundamental and controversial issue has been the chemical structure of N atoms within the oxynitride film and at the SiO_2/Si interface,[5,6,12] which is crucial to characterize and understand the microscopic structures and processes of N incorporation. Our recent high-resolution N 1*s* photoemission investigation clarified the chemical bonding configuration of the N atoms in the thermally-nitrided oxynitrides films. In that case, the N species is uniquely in the $N{\equiv}Si_3$ bonding state, but those in the Si-rich interfacial layers and in the O-rich SiO_2 matrix have different N 1*s* binding energy due to the second-nearest-neighbor effect.[13] This chemical state is the major and common N bonding state for most of the oxynitride films prepared through various different processes.

In the present work, we focus on the nitrogen bonding states within the silicon oxynitride films prepared by a plasma process (denoted as plasma SiON hereafter). This provides a chance to study the process dependence of the N incorporation and also other possible N bonding structures beyond the ubiquitous $N{\equiv}Si_3$ state. Indeed, the previous photoemission studies on plasma oxynitride observed a few different high-binding N 1*s* features in addition to those observed for thermal oxynitrides. However, the chemical origins and the physical properties, such as the thermal stability, of these N species have not been clear.

We apply high-resolution core-level photoemission using synchrotron radiation for the first time to plasma SiON. The films studied here are ultrathin films of 1–2 nm thickness as used in the up-to-date device applications. These ultrathin films are useful in avoiding the extra charging effect of a thicker dielectric film. The rich N chemical structures, especially the N—O and $N{=}O_2$ states, are revealed unambiguously by high-resolution N 1*s* spectra. The qualitative depth distributions and the thermal stability of various different bonding states are detailed. In particular, the present result differentiates the transient and the (quasi-) stable N chemical states, which would be relevant to the physical and device properties of the silicon oxynirides.

II. EXPERIMENT

The ultrathin oxynitride layers are prepared using N_2-plasma nitridation of ultrathin SiO_2 films on Si(100) with

300 W rf power at low (190 °C) and high (410 °C) substrate temperatures (LT- and HT-plasma SiON, respectively). A thermal oxynitride film is also prepared as a reference by exposing NO on a similar SiO_2 film at 850 °C. The ellipsometry measurements indicate that the thickness of the oxynitrides is in the range of 11–17 Å.

Before the high-resolution photoemission study using synchrotron radiation, we performed standard x-ray photoelectron spectroscopy (XPS) measurements using monochromatic Al $K\alpha$ emission to estimate the nitrogen concentration within the SiON layers. It is estimated to be approximately 3–5% from the intensities of O 1*s* and N 1*s* peaks of the XPS spectra after an atomic sensitivity correction. The N 1*s* spectra from the above measurements indicate a dominant and broad peak at around 398 eV for all SiON samples but with some additional structures toward higher binding energies for the plasma SiON. Although this result is consistent with the earlier results,[5,6] it is far from being sufficient to explain the chemical details for the incorporated N species.

For such a purpose of investigating the further details of the chemical bonding structures of nitrogen, the synchrotron radiation photoemission experiments were performed on a high-brightness soft x-ray beam line (8A1) connected to an undulator (U7) at the Pohang Accelerator Laboratory (PAL) in Korea.[13] N 1*s* core-level spectra were obtained using photon energies ($h\nu$'s) in the range of 430–600 eV to achieve depth-dependent nitrogen profiles. All spectra are taken using a high performance electron analyzer (SES-2002, Gamma Data, Sweden) with an overall instrumental resolution (the analyzer and the photon beam in total) of 350 meV for N 1*s*. All the measured spectra are normalized to the background intensities of the low-binding energy-side of the N 1*s* peaks. The decomposition of all N 1*s* photoelectron spectra is accomplished through a standard least-square fitting scheme using a Gaussian-Lorentzian function. The binding energies were calibrated by referring the position of the Si $2p_{3/2}$ level of bulk Si atoms at 99.20 eV.[13]

III. RESULTS AND DISCUSSION

Figure 1 shows the N 1*s* spectra for the three oxynitride films described above. The spectra are taken at $h\nu = 560$ eV in normal emission from the samples without any post-annealing treatment. The raw spectra for the three oxynitride films show clear variations in the line shape as well as the peak maxima, suggesting that there are significant differences in the nitrogen profiles, not only between the thermal SiON and plasma SiON, but also between the two different plasma SiON. For the thermal SiON, one can distinguish a well-defined peak at 397.5 eV and some weak features toward higher binding energies. However, the raw spectra for the plasma SiON show peak maxima at 398.9 eV and strong shoulders at 397.5 eV (and also at 400.5 eV for LT-plasma SiON) with some other weak features. From the inspection of the raw spectra, it can be said that there are at least three major nitrogen species represented by the N 1*s* components at 397.5, 398.9, and 400.5 eV, which are denoted as N1, N3, and N5, respectively. A very minor high binding feature (denoted as N6) is also noticeable from the raw spectra around 402.5 eV commonly for all three spectra.

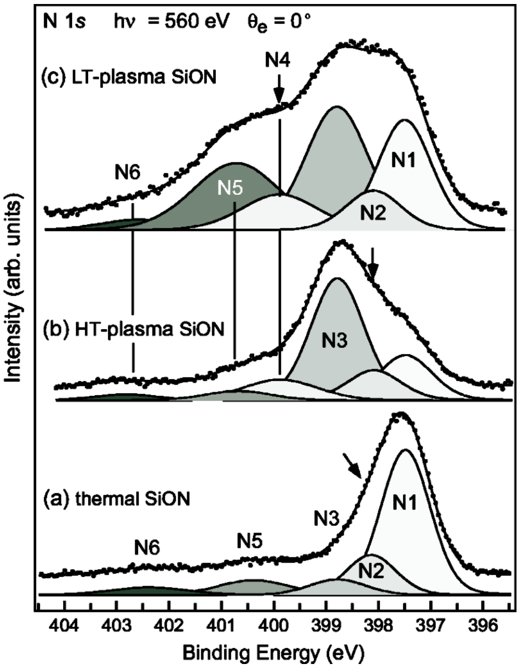

FIG. 1. N 1*s* photoelectron spectra taken at $h\nu = 560$ eV for (a) the thermal SiON, (b) the HT(410 °C)-plasma SiON, and (c) the LT(190 °C)-plasma SiON. The peak decompositions through standard curve-fitting analyses are given together, where the solid lines superimposed on the raw data (dots) are the results of the fits.

For a more detailed and quantitative analysis, a careful decomposition procedure is applied to all spectra, whose results are shown in Fig. 1. This curve-fitting analysis discloses that there are two other nontrivial components at 398.2 ± 0.1 (N2) and 400.0 ± 0.2 eV (N4). As indicated by the arrows in Fig. 1, the N2 component constitutes the asymmetric line shape towards a high binding energy for N 1*s* of the thermal SiON but is overlapped by N1 and N3 for the plasma SiON. The N4 component is barely identified from the raw spectra of LT-plasma SiON between N3 and N5 [see the arrow in Fig. 1(c)]. The N 1*s* line shape of the plasma SiON cannot be reproduced without these two components. The binding energies for N1, N3, and N5 are precisely determined to be 397.5 ± 0.1, 398.9 ± 0.1 (N3), and 400.6 ± 0.3 eV (N5), respectively. The full-width-at-half-maximum values are optimized to 1.2 ± 0.05 eV for N1 and N2, 1.4 ± 0.05 eV for N3, and 1.8 ± 0.05 eV for N4-N6.

For the thermal SiON, the only distinguished peak is N1 with the other major component N2. This double component structure for the thermal SiON was fully characterized by our previous study.[13] Both components are unambiguously related to the N species with three Si nearest neighbors ($N \equiv Si_3$).[4,13–17] The N2 species is different from N1 only in the second-nearest neighbors, where the oxygen atoms substituting Si ($N[-SiO_3]_x$) induce the binding energy difference of 0.7 eV.[13,14,18,19] That is, N2 corresponds to the nitrogen atoms dispersed within the SiO_2 matrix, while N1 corresponds to those incorporated into the Si interfacial layers.[20] This is also supported by the qualitatively different depth distribution of the two N species.[13] In addition to these major nitrogen species, the present result indicates that three other mi-

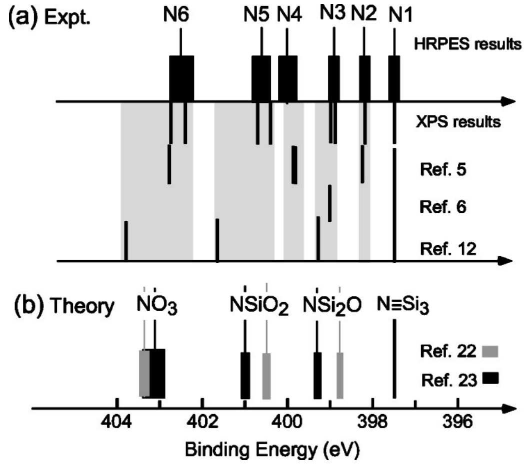

FIG. 2. (a) Summary of N 1*s* binding energies from the present and the previous experiments (Refs. 5, 6, and 12). (b) The results of the recent theoretical calculations (Refs. 22 and 23). All binding energies are referred from that of bulk Si $2p_{3/2}$ at 99.20 eV.

nor nitrogen species such as N3, N5, and N6 are present for this specific thermal SiON. These species were not found for the thermal SiON after high temperature rapid thermal process as in our previous study.[20] We thus assign these high binding energy species to the unstable and transient nitrogen species for which more extensive discussion is given below.

The dominant and characteristic component for plasma SiON is the N3 peak at 398.9 eV [see Figs. 1(b) and 1(c)], in clear contrast to N1 of thermal SiON. Another characteristic feature is N5 especially for LT-plasma SiON prepared at a low temperature of 190 °C. Similar high-binding spectral features were observed in the previous XPS experiments on the plasma oxynitrides at binding energies of around 399, 400, 402, 403, and 404 eV, which were mainly related to the oxidized nitrogen species.[5,6,9,12,21] However, there have been quantitative disagreements in the binding energy of each specific N species, which have made the assignment of its origin uncertain. Such disagreements could be partly due to the experimental difficulties given by the relatively low sensitivity and limited spectral resolution of the conventional XPS measurements. Moreover the varying thicknesses of the SiON films could have resulted in the different binding energies of a similar spectral feature due to the different core-hole screening.[13] Therefore, a high-resolution measurement on the very thin film is necessary, as in the present experiment, along with a systematic comparison of the binding energies from different experiments and theoretical calculations.

Figure 2 summarizes the N 1*s* binding energies obtained from the previous XPS experiments[5,6,12] as well as the present high-resolution measurement and the theoretical expectations.[22,23] From the comparison of the present result and the theoretical calculations,[22,23] it is natural and straightforward to assign the two characteristic and major spectral features N3 and N5 to $\mathrm{O{-}N{=}Si_2}$ and $\mathrm{O_2{=}N{-}Si}$ species, respectively, with a very good agreement with the theoretical results.[22,23] Although the agreement is not quantitative, we may safely attribute N6 to a higher oxidation state of $\mathrm{O_3{\equiv}N}$, too. The two previous XPS studies[6,12] reported consistent binding energies for the $\mathrm{O{-}N{=}Si_2}$ (N3) species, although the other[5] reported a much higher binding energy of 399.8 eV. This value is located in the middle of those for $\mathrm{O{-}N{=}Si_2}$ and $\mathrm{O_2{=}N{-}Si}$ and corresponds to that of N4 in the present study. This point is discussed below. We further note that the XPS measurement for a very thick SiON film[12] indicated a slightly higher binding energy for N3 in comparison with the very thin film of the present study. This may be understood from the enhanced core-hole screening effect and/or to the change of the second-nearest neighbor configuration in a thicker $\mathrm{SiO_2}$, which is different from the charging effect, leading to not a relative but an overall shift of the whole spectrum.[20,24,25] The previous assignment of the binding of the $\mathrm{O_2{=}N{-}Si}$ species (N5) was also done on such a thick film[12] and reported a considerably higher binding energy than the present one, consistent with the core-hole screening effect. The same argument holds for the case of the binding energy and assignment of $\mathrm{O_3{\equiv}N}$ (N6) as shown in Fig. 2. In summary of this comparison, we conclude that the present measurement on an extremely thin film and the previous study on a very thick film give roughly the lower and upper bounds for the binding energy values of the oxidation states of nitrogen within the $\mathrm{SiO_2}$ matrix (as indicated by the grey bars in Fig. 2), which are fully consistent with the theoretical expectations.

Within the above assignment scheme, what is left unassigned is the peak observed at around 400 eV (N4) in the present study and in that of Ref. 5. We cannot resort to the core-hole screening effect with a different film thickness in order to relate N4 to $\mathrm{O{-}N{=}Si_2}$, since the assignments of the other peaks of the same study is quantitatively consistent with the present ones. We thus suggest that this component can be due to yet another chemical configuration, which was not mentioned above. One candidate is the molecular $\mathrm{N_2}$ species trapped within the oxide matrix. In fact, the high density $\mathrm{N_2}$ plasma employed in this study produces mostly energetic molecular $\mathrm{N_2}$ species (such as $\mathrm{N_2}$ radicals) in addition to atomic nitrogen species. Some of those energetic $\mathrm{N_2}$ species impinging onto the $\mathrm{SiO_2}$ layers may be incorporated without breaking their $\mathrm{N{-}N}$ bonds. In support of this idea, a recent near-edge x-ray absorption study observed clear evidence of the existence of the molecular $\mathrm{N_2}$ species within a plasma-treated SiON film.[26]

In spite of such common spectral features, there are large differences in the relative abundance of the various N components between the LT- and HT-plasma SiON. One major difference is the relative intensities of N1 and N5 (as being normalized by that of N3), which is significantly higher for LT-plasma SiON. As shown below, the N5 component is a very surface-sensitive one indicating that the corresponding N atoms are localized near the topmost layer. Thus the intensity difference for this component rather directly represents the population of the corresponding N species on the surface. The other major difference is the N1/N3 intensity ratio. However, the difference in N1/N3 can largely come from the difference in the oxide thickness since a thicker oxide would attenuate the N1 intensity from the N species located at the $\mathrm{SiO_2/Si}$ interface.[27]

After establishing the chemical origin of the characteristic N species of the plasma SiON, we discuss the thermal sta-

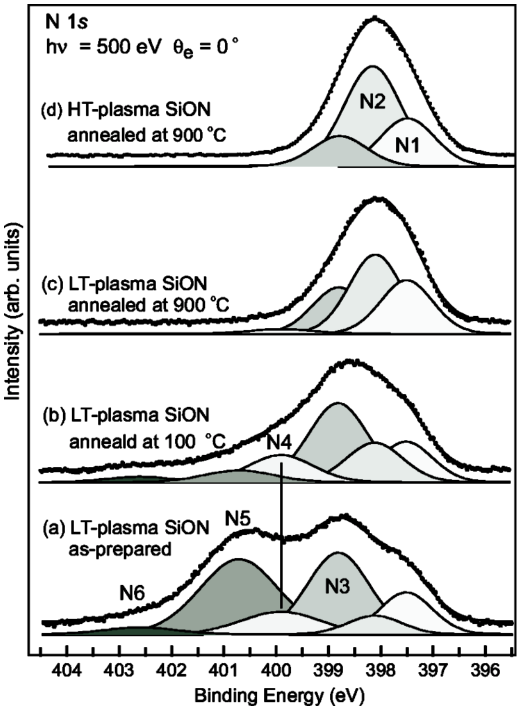

FIG. 3. N 1*s* photoelectron spectra taken at $h\nu = 500$ eV for LT(190 °C)-plasma SiON (a) without or (b)–(c) with further annealings and (d) HT(410 °C)-plasma SiON annealed at 900 °C.

bility of each species. The thermal stability can be explored by examining the evolution of the corresponding N 1*s* components for the post-annealings with increasing temperature. Figure 3 shows the N 1*s* core-level spectra taken at $h\nu = 500$ eV for the plasma SiON after post-annealing treatments. The raw spectrum in Fig. 3(a) for LP-SiON shows three distinct structures, which correspond to the important N species of N1, N3, and N5. After a mild annealing at a temperature of as low as 100 °C, the N5 component at 400.5 eV almost disappears and instead the intensity of N2 increases [Fig. 3(b)]. A further annealing at a much higher temperature of 900 °C results in the complete reduction of N4, N5, and N6 and the further increase of N2. At this temperature the N3 component is also decreased significantly. A very similar trend is found also for the HT-plasma SiON as shown in Fig. 3(d), which is to be compared with Fig. 1(c); mainly the increase of N2 at the expense of N3 with an annealing at 900 °C. In this case the contribution of the N4-N6 components is only marginal but the complete disappearance of them at 900 °C is fully consistent with the case of LT-plasma SiON. After the 900 °C-annealing the overall shape of N 1*s* is very similar between LT- and HT-plasma SiON. It should also be noted that the intensity of N1 is affected very limitedly by the annealing up to 900 °C.

The above results clearly show that the N species of N4-N6 are thermodynamically unstable and do not exist above 900 °C. Especially, the $O_2{=}N{-}Si$ (N5) species is very volatile as is greatly affected by even 100 °C annealing. Note also that the desorption of nitrogen species is not significant at this temperature range. Instead, these highly-oxidized species of $O_2{=}N{-}Si$ (N5) and $O_3{\equiv}N$ (N6) seem to convert into the stable species of $N{\equiv}Si_3$ (N2) but not into $O{-}N{=}Si_2$ (N3). In contrast to the N5 and N6 species, the N3 ($O{-}N{=}Si_2$) species partly survives the high temperature annealing although the population of N3 decreases gradually as the substrate temperature approaches 900 °C. The N3 ($O{-}N{=}Si_2$) species also seems to convert into the stable $N{\equiv}Si_3$ (N2) species during the annealing treatments. It is notable that the N1 component (the interfacial $N{\equiv}Si_3$ species) has only a very marginal change in its intensity with post-annealing. This means that the conversion of oxidized N species into $N{\equiv}Si_3$ does not accompany an interdiffusion over the interface to reach the Si-rich layers. This could be possible if (i) there exists significant interfacial diffusion barrier or (ii) the possible interfacial $N{\equiv}Si_3$ sites are already saturated. We further suggest that in either of the above cases the preexisting N species has a major role since the initial interfacial nitridation of a pure SiO_2 layer is possible even at 700 °C.[6]

The present results also agree well with our previous photoemission studies, which showed that the $N{\equiv}Si_3$ species (N1 and N2) are the only stable species for the thermal-SiON films formed at 1050 °C.[13] It is likely that the N3 species decomposes completely into N1 or N2 at a higher temperature than 900 °C. For the present study, however, we focus on the evolution of each N species only up to 900 °C, since (i) the typical device processes employ thermal treatments less than 900 °C and (ii) a higher temperature annealing in UHV yields a very rough surface.

The issue of interdiffusion during the post-annealing and also the further characterization of each N species require the depth information of a given species. We qualitatively studied the relative depth distribution of the N species in two different ways; (i) changing the mean free path (the kinetic energy or the emission angle) of N 1*s* photoelectrons and (ii) etching chemically the oxide film by HF. For example, Fig. 4 shows the N 1*s* spectra for LT-plasma SiON annealed at 600 °C taken at two different photon energies of 500 and 560 eV. Obviously, there are apparent variations in the lineshape, which results in a noticeable shift of the apparent peak maximum. N1 loses its intensity compared with those of N2-N4 at a lower photon energy of $h\nu = 500$ eV or at a more surface-sensitive kinetic energy.[13] The variations of the intensity of each N species from Fig. 4(a) as well as for the thermal SiON are compared by the corresponding intensity ratios as in Fig. 4(b). The results indicate that the different N species have distinctively different depth profiles with increasing depths from the bulk in the order of N1, N2/N3, N4, N5/N6. This depth-dependent change of the spectra was consistently observed with a systematic variation of the emission angle, indicating the possible photoelectron diffraction to be marginal.

We further corroborate the above result from the selective etching of the oxide layers. The chemical etching in a dilute HF solution is a widely used method for selectively removing the SiO_2 layers primarily utilizing the high etching selectivity of SiO_2 to the Si substrate. Figure 5 shows the corresponding N 1*s* spectra for HT-plasma SiON and themal SiON after HF etching. As indicated from the Si 2*p* spectra in the insets, the SiO_2 layer is almost completely removed. Both N 1*s* spectra exhibit a very similar spectral shape after the etching, which are composed mainly of N1. One can

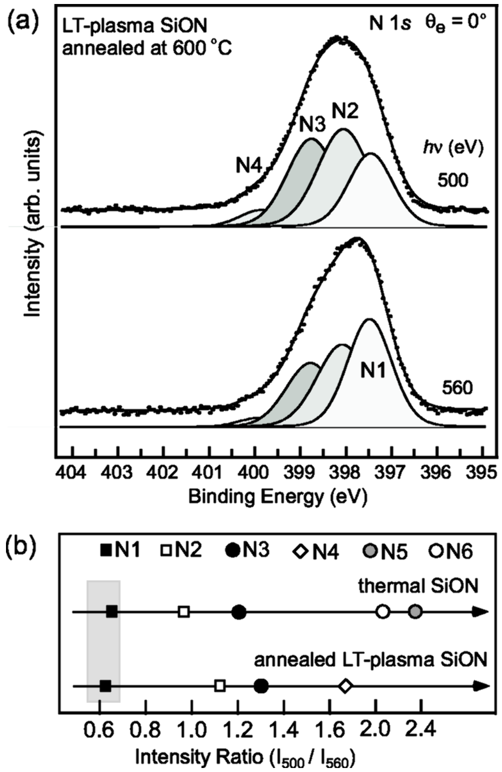

FIG. 4. (a) N 1*s* core-level spectra taken at $h\nu$'s of 500 and 560 eV for the LT(190 °C)-plasma SiON after post-annealing at 600 °C. (b) The ratios of the N 1*s* intensities taken at two photon energies for the LT-SiON after the post-annealing as well as for the thermal SiON are compared.

conclude that N1 corresponds to the nitrogen atoms which are incorporated within the Si layers, that is, below the SiO_2-Si interface before the etching, while the other N components are distributed within the SiO_2 matrix. The small N2 as well as the features above 400 eV are tentatively assigned as due to the result of a partially nonuniform etching of the SiO_2 layers or side reactions of nitrogen atoms during the chemical etching process. This result is consistent with the depth information given above and also with our recent suggestion of the structure of the incorporated N atoms within the Si subsurface layers.[20]

IV. CONCLUSION

We investigate the local bonding configurations of nitrogen species incorporated into the ultrathin SiO_2 layers on Si(100) by N_2-plasma nitridation. High-resolution photoelectron spectroscopy using synchrotron radiation is utilized. From the systematic analysis of the highly-resolved N 1*s* photoelectron spectra, it is shown that there are at least four different N chemical states. Through a systematic comparison of the corresponding N 1*s* binding energies with the previous experimental and theoretical studies, we could reliably assign these N chemical states to $O_2{=}N{-}Si$, $O{-}N{=}Si_2$, $N{\equiv}Si_3$ within the SiO_2 matrix and $N{\equiv}Si_3$ within the interfacial Si layers with binding energy shifts of 3.1, 1.4, 0.7, and 0 eV, respectively. In particular, the occurrence of the oxidized N species of $O_2{=}N{-}Si$ and $O{-}N{=}Si_2$ is characteristic for the N_2 plasma process in clear contrast to the high temperature thermal (oxy)nitridation. The portions of the N species with higher oxidation states increases at a lower substrate temperature. These oxidized N species, especially the $O_2{=}N{-}Si$ species, are very much unstable thermally, which readily converts into the stable $N{\equiv}Si_3$. However, very interestingly, the $O{-}N{=}Si_2$ is significantly more stable than $O_2{=}N{-}Si$, which even partly survives a thermal annealing at a temperature of as high as 900 °C. It is also found that the oxidized species are formed mostly near the surface or the shallow part of the oxide film. These observations indicate clearly that the oxidized N atoms formed by energetic and reactive nitrogen plasma species are not thermally stable but is kinetically trapped. In addition, it is shown that the thermal conversion of the oxidized N species into the stable $N{\equiv}Si_3$ occurs within the SiO_2 film not reaching down to the interfacial Si layers. This suggests that the preincorporated interfacial N atoms block the diffusion of N atoms across the SiO_2/Si interface. Since a significant population of the N—O species remain within the film even after a heavy thermal annealing at 900 °C, the difference in electrical and device properties between the thermal and plasma SiON films can be related at least partly to this specific chemical species. A further theoretical study is desirable for the understanding of the different stability of the N—O and $N{=}O_2$ species.

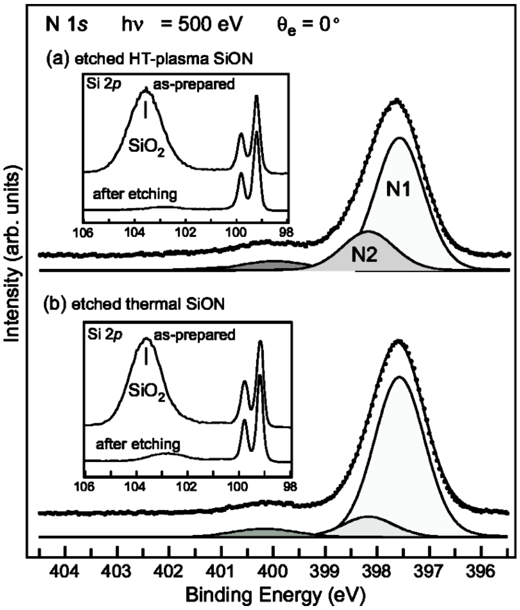

FIG. 5. N 1*s* core-level spectra taken at $h\nu$=500 eV for (a) the HT(410 °C)-plasma SiON and (b) the thermal SiON after chemical etching in the 50:1 HF solution. Si 2*p* core-level spectra taken at the same photon energy are also given in the insets.

This work was supported by Hynix Semiconductor Inc., Yonsei University and MOST (through Center for Atomic Wires and Layers within the CRi program). PAL is supported by MOST and POSCO.

*Author to whom all correspondence should be addressed. Electronic address: yeom@phya.yonsei.ac.kr

[1] E. C. Carr and R. A. Buhrman, Appl. Phys. Lett. **63**, 54 (1993).
[2] Z.-Q. Yao, H. B. Harrison, S. Dimitrijev, D. Sweatman, and Y. T. Yeow, Appl. Phys. Lett. **64**, 3584 (1994).
[3] M. L. Green, D. Brasen, K. W. Evans-Lutterodt, L. C. Feldman, K. Krisch, W. Lennard, H.-T. Tang, L. Manchanda, and M.-T. Tang, Appl. Phys. Lett. **65**, 848 (1994).
[4] A. Kamath, D. L. Kwong, Y. M. Sun, P. M. Blass, S. Whaley, and J. M. White, Appl. Phys. Lett. **70**, 63 (1997).
[5] J. R. Shallenberger, D. A. Cole, and S. W. Novak, J. Vac. Sci. Technol. A **17**, 1086 (1999).
[6] H. Kobayashi, T. Mizokuro, Y. Nakato, K. Yoneda, and Y. Todokoro, Appl. Phys. Lett. **71**, 1978 (1997).
[7] P.-C. Chen, K. Y.-J. Hsu, J.-Y. Lin, and H.-L. Hwang, Jpn. J. Appl. Phys., Part 1 **34**, 973 (1995).
[8] Y. Saito, Appl. Phys. Lett. **68**, 800 (1996).
[9] S. R. Kaluri and D. W. Hess, Appl. Phys. Lett. **69**, 1053 (1996).
[10] S. B. Kang, S.-O. Kim, J.-S. Byun, and H. J. Kim, Appl. Phys. Lett. **65**, 2448 (1994).
[11] R. I. Hegde, P. J. Tobin, K. G. Reid, B. Maiti, and S. A. Ajuria, Appl. Phys. Lett. **66**, 2882 (1995).
[12] J. P. Chang, M. L. Green, V. M. Donnelly, R. L. Opila, J. Eng, Jr., J. Sapjeta, P. J. Silverman, B. Weir, H. C. Lu, T. Gustafsson, and E. Garfunkel, J. Appl. Phys. **87**, 4449 (2000).
[13] J. W. Kim, H. W. Yeom, Y. D. Chung, K. Jeong, and C. N. Whang, Phys. Rev. B **66**, 035312 (2002).
[14] Y. D. Chung, J. W. Kim, C. N. Whang, and H. W. Yeom, Phys. Rev. B **65**, 155310 (2002).
[15] N. Miyata, H. Watanabe, and M. Ichikawa, Appl. Phys. Lett. **76**, 3561 (2000).
[16] H. C. Lu, E. P. Gusev, T. Gustafsson, E. Garfunkel, M. L. Green, D. Brasen, and L. C. Feldman, Appl. Phys. Lett. **69**, 2713 (1996).
[17] Z.-Q. Yao, J. Appl. Phys. **78**, 2906 (1995).
[18] Y. K. Kim, J. R. Ahn, W. H. Choi, H. S. Lee, and H. W. Yeom, Phys. Rev. B **68**, 075323 (2003).
[19] G. F. Cerofolini, A. P. Caricato, L. Meda, N. Re, and A. Sgamellotti, Phys. Rev. B **61**, 14 157 (2000).
[20] J. W. Kim, H. W. Yeom, K. J. Kong, B. D. Yu, D. Y. Ahn, Y. D. Chung, C. N. Whang, H. Yi, Y. H. Ha, and D. W. Moon, Phys. Rev. Lett. **90**, 106101 (2003).
[21] M. Bhat, J. Ahn, D. L. Kwong, M. Arendt, and J. M. White, Appl. Phys. Lett. **64**, 1168 (1994).
[22] M. Takahashi, T. Mizokuro, Y. Nishioka, and H. Kobayashi, Surf. Sci. **518**, 72 (2002).
[23] G.-M. Rignanese, A. Pasquarello, J.-C. Charlier, X. Gonze, and R. Car, Phys. Rev. Lett. **79**, 5174 (1997).
[24] S. Iwata and A. Ishizaka, J. Appl. Phys. **79**, 6653 (1996).
[25] H. W. Yeom, H. Hamamatsu, and R. I. G. Uhrberg, Phys. Rev. B **59**, R10 413 (1999).
[26] H. J. Shin *et al.*, (unpublished data.)

[27] The ellipsometric measurements indicate that the oxide thickness for the LP-SiON is 11 Å, which is significantly thicker than 17 Å of HP-SiON. The corresponding N1 intensity for HP-SiON can be attenuated to one-third of that for LP-SiON, when we consider the typical attenuation length of 5–10 Å at the kinetic energy range used.